Mode I and II fracture behaviour of steel fibre reinforced high strength geopolymer concrete: an experimental investigation

T.S. Ng, T.N.S. Htut & S. J. Foster
School of Civil and Environmental Engineering, The University of New South Wales, Australia.

ABSTRACT: In this paper, results are reported for a series of discrete fibre pullout tests from high strength geopolymer concrete and high performance, reactive powder, concrete. The results are also compared to that of discrete fibres pulled out from conventional strength mortar. The tests cover both Modes I and II fracture and a number of different fibre angles to the separation plane were studied. The results show that with provision of an end hook the bond is too great and the fibres fracture, even for high strength short fibres. It was found that the mechanical anchorage due to the snubbing effect is especially important and that in the Mode II tests, fibres at negative angles smaller than -30 degrees are largely ineffective over the engineering range of separation, or crack, plane openings.

1 INTRODUCTION

Geopolymer concrete is an inorganic polymer concrete, containing no ordinary Portland cement (OPC). It is produced by reacting aluminosilicate source material with alkaline solution.

Geopolymer concrete is more environmental friendly than that of OPC concrete. Concrete made of geopolymer poses excellent mechanical properties and has high early age strength. Geopolymer can gain 70 % of the final compressive strength in the first four hours of setting (Li. et al. 2004). Hardjito & Rangan (2005) developed a fly ash based geopolymer concrete with an achievable compressive strength ranging from 8 MPa to 90 MPa, depending on the mix composition and curing method. Geopolymer concrete has also been found to be more durable than OPC concrete. Comparing with OPC concrete, geopolymer concrete has little shrinkage, low creep and superior chemical resistance (Wallah & Rangan, 2006, Gourley & Johnson 2005).

Like other cementitious composites, geopolymer concrete is brittle, with low tensile strength and strain capacity. The use of fibres as a reinforcement in cementitious composites is common and serves the purpose of both increasing the tensile strength and improve post-cracking behaviour of the material with the fibres bridging the crack openings (Gopalaratnam & Shah 1987, Guerrero & Naaman 2000).

In fibre reinforced cementitious composites, the resistance to crack propagation depends on the bond resistance of the fibre that, in-turn, depends on the mechanical properties of the matrix and of the fibres such as geometry, orientation and length. For randomly orientated fibre reinforced composites, not all fibres are aligned in the direction of the applied load; instead, almost all fibres lie at an angle to the loading direction. In such cases, fibres are subjected to a combination of shear, bending and tensile stresses (Bartos & Duris 1994). Due to their inclination angles, fibres bend at the exit point (i.e. at the crack interface) with snubbing of the fibres and spalling of the matrix expected for fibres at high inclination angles (Morton & Groves 1974). The importance of the snubbing effect when fibres are pulled out from a cementitious matrix are highlighted by many researchers (Li 1992, Naaman & Najm 1991, Robins et al. 2002 & others). Lee & Foster (2006a) and Htut & Foster (2008) also provided an insight of the snubbing effect in Mode I & II fracture using radiographic imaging. Space in this paper prohibits an extensive review of the literature on Mode I & II fracture of fibre reinforced cementitious composites but more information on the topic can be found in Voo & Foster (2004) and Lee & Foster (2006b).

Insight of fibre behaviour during pullout is vital for developing a constitutive model for fibre reinforced concrete. There is no easy method to determine fibre pullout micromechanics other than undertaking experimental discrete fibre pullout test. The pullout test allows observation and understanding of all stages of pullout process starting from the initial elastic deformation the fibre been pulled-out or fractured.

As a potential alternative to OPC concrete, the understanding, to date, on fibre bond behaviour in geopolymer concrete is lacking. This research investigates the fibre pullout mechanism in geopolymer concrete subjected to mode I and II actions and a comparison is made with ordinary cement matrix and

reactive powder concrete (RPC). In the framework of this experimental study, the pullout resistance due to the influence of different fibre inclination angles and fibre types (end-hooked and straight) were investigated.

2 EXPERIMENTAL PROGRAM

2.1 Introduction

The details of the uniaxial tension tests and direct shear tests are described in this section. Two series of experiments were undertaken; uniaxial tension (Mode I) and direct shear (Mode II) with straight (ST) and end-hooked (EH) fibres. Different fibre inclination angles were investigated for each series. Three different type of cementitious matrixes (geopolymer concrete, RPC, ordinary cement mortar) were used as the pullout medium.

2.2 Materials and specimen preparation

Figures 1 and 2 show the specimen dimensions for the Mode I fracture and Mode II fracture specimens. The discrete fibre pullout and push-off specimens were fabricated in two separate geopolymer concrete pours. The fibre inclination angle (θ) is measured from a horizontal line drawn normal to the interface of the two halves of the specimen. In the L-shaped direct shear specimens, a clockwise direction is considered as positive in the "2" configuration whereas an anticlockwise direction is negative. For example, the inclination angle shown in Figure 2 is positive.

For the Mode I tests, a single row of four fibres were clamped into position for the first pour using a specially fabricated steel fibre clamp placed on the side of the specimen selected for the second pour. After the first pour, the steel clamp was released and the second side of the specimen was cast. A telfon sheet was inserted in between the two halves of the specimen at the steel fibre clamp to ensure that there is no adhesion between the two halves of the specimens and the applied force is transferred solely through the fibres. The thickness of the tensile discrete fibre pullout specimens was 30 mm.

The direct shear (double L-shaped) specimens were constructed in a similar manner to the tensile specimens with four fibres clamped into position on one side of the specimen while the geopolymer concrete was cast on the other. Telfon sheet was placed along the shear plane to create a smooth frictionless surface when conducting the test. The thickness of the specimens was 40 mm.

The geopolymer concrete mix used in the specimens was composed of kiln dried Sydney sand and fly ash from Eraring Power Station in NSW, ground granulated blast furnace slag, Kaolite high perform-

ance ash (HPA) from Callide Power Station in Queensland Australia and alkaline activator. The mix proportion is given in Table 1. Table 2 presents the chemical compositions of the fly ashes and slag. The alkaline activator was comprised of Sodium hydroxide (NaOH) solution with a concentration of 12M and sodium silicate solution (with Na_2O = 14.7 %; SiO_2 = 29.4 %; and H_2O = 55.9 % by mass).
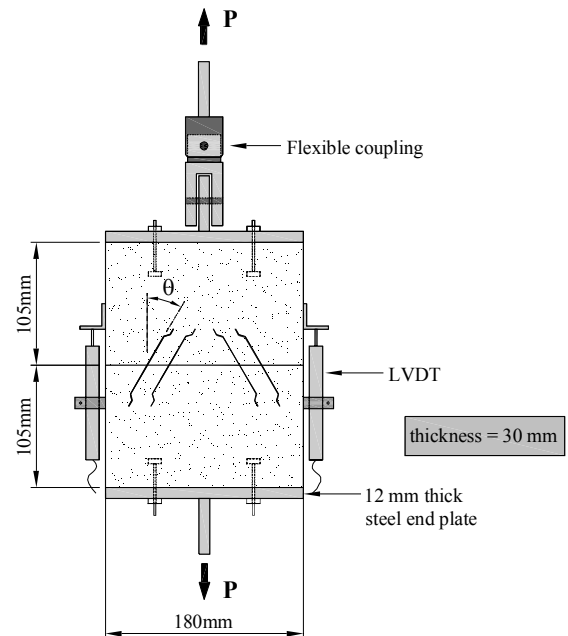
Figure 1. Testing arrangements for tensile specimen.
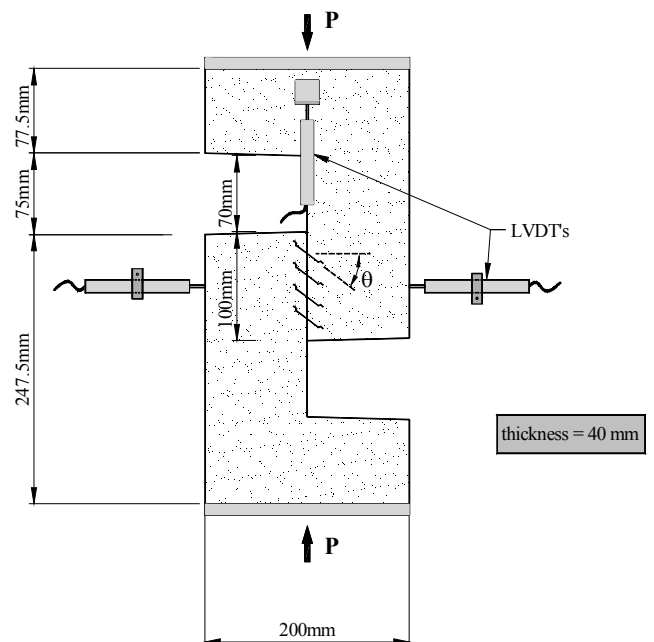
Figure 2. Testing arrangements for direct shear specimen.

The ratio of NaOH solution to sodium silicate solution was 1:2.5 by mass. The activator was blended and stored for at least 24 hours prior to the manufacturing of the geopolymer concrete as it was reported by Hardjito & Rangan (2005) that this enhances the polymerization process and prevents bleeding and

segregation of the fresh concrete. No other additives were used in the mix design.

Table 1. Geopolymer Concrete Mix Composition.

Materials	Sand	Fly ash	Slag	Kaolite HPA	Alkaline Activator
% by mass	39.2	29.4	5.9	3.9	21.6

Table 2. Chemical composition of fly ash (by mass %).

Element	Fly Ash	Slag	Kaolite HPA
SiO_2	66.56	31.52	45.14
Al_2O_3	22.47	12.22	33.32
Fe_2O_3	3.54	1.14	11.99
CaO	1.64	44.53	4.13
K_2O	1.75	0.33	0.13
Na_2O	0.58	0.21	0.07
MgO	0.65	4.62	1.37
MnO	0.06	0.36	0.23
P_2O_5	0.11	0.02	0.56
TiO_2	0.88	1.03	2.19
SO_3	0.10	3.24	0.48
LOI*	1.66	0.79	0.41

Note: * LOI = Loss on ignition

The mortar mix used in the specimens was composed of kiln dried Sydney sand and general purpose Portland cement mixed in a ratio of 3:1 (sand : cement) and water at a water : cement ratio of 0.4. No other additives used in the mix design.

The components of reactive powder concrete (RPC) used was general Portland cement, undensified silica fume, and Sydney Sand. The superplasticizer used in the mix was Glenium 51 and the water binder ratio was 0.22.

The deformed steel fibres chosen for this study were end-hooked (EH) Dramix® cold drawn wire fibres produced by Bekaert and high yield strength EH fibre provided by Dura Technology of Malaysia. The ST steel fibres used in this study were made from EH fibres with the hook portions removed. The fibre dimensions and material properties are given in Table 3.

Table 3. Properties of steel fibres.

Fibre Type	Dramix® RC-65/35-BN		Fibre by Dura Technology
Fibre Type	Hook	Straight	Hook
Diameter, d (mm)	0.55	0.55	0.3
Length, l (mm)	35	23 or 28	25
Aspect Ratio, l/d	64	42 or 51	83
Tensile Strength, σ_{fu} (MPa)	1340	1340	2300

Details of the test series are presented in Table 4 with the specimens being designated using the notation XX±θYY- Z (c) where XX = UT for the "uniaxial tension" and XX = DS for the "direct shear" tests, ±θ is the fibre inclination angle, Y is the fibre type (EH = end-hooked fibres and ST = straight fibres), Z is the pullout medium (M = cement mortar, G = geopolymer and R = RPC matrix) and (c) = fibre length. For example, UT±45EH-G (35) is a uniaxial tension

test with 35 mm EH fibres at an inclination angle of 45° and pullout medium is geopolymer. For all series, the fibres were embedded at equal length on each side of the separation plane, i.e. embedment ratio of 1:1.

Table 4. Specimen properties.

Test Specimen Series	θ (degree)	Mean Compressive Strength, f_{cm} (MPa)	Elastic Modulus E_c (GPa)
UT±θEH-M (25)	0, 30, 60	41	27
UT±θEH-M (35)	0, 30, 60	38	24
UT±θST-M (23)	0, 30, 60	40	27
UT±θEH-G (35)	0, 15, 30, 45, 60	90	19
UT±θST-G (28)	0, 15, 30, 45, 60	94	19
UT±θEH-R (25)	0, 15, 30, 45, 60	148	40
DS±θEH-G (35)	+30, 0, -15, -30, -45, -60	90	19
DS±θST-G (28)	+30, 0, -15, -30, -45, -60	94	19

The specimens were cast horizontally in two stages into the moulds. The first stage involved casting a section on one side of the separation plane, with the other half of the specimen blocked out and the fibres protected between two steel sandwich blocks (fibre clamp). After setting of the first half of the specimen, the steel clamps were removed from the second half of the specimen and the remaining half was cast. Six 200 mm high by 100 mm diameter cylinders were cast with each half of the specimen for quality control.

For geopolymer and RPC matrix, after setting of the second half of the specimen, the specimens and cylinders were stripped and placed in a hot water bath at 90°C for seven days. For the cement mortar matrix, the specimens were placed in the fog room for minimum of 28 days for curing. The specimens were left in the laboratory environment after curing and until testing.

2.3 Testing arrangements

The testing setup and arrangements for uniaxial tensile (Mode I) and direct shear (Mode II) tests are similar to those of Foster et al. (2007) and are shown in Figures 1 and 2 respectively. The tests were conducted on a 10 kN Instron universal testing frame. Two linear variable differential transducers (LVDTs) were used to measure the displacements in the direction of movement of the loading jacks. Loading was conducted using displacement control at a rate of 0.2 mm per minute until the peak value was attained. The rate was then increased to a minimum of 0.1 mm

per minute, with further rate increases introduced as necessary during the test. Each test specimen was loaded until fibres were either pullout completely from the section or fractured. Load and displacement readings were recorded at 0.2 second intervals. For the mode II test, additional two LVDTs were used to measure the separation plane opening displacement.

The mean cylinder compressive strength at the time of testing is given in Table 4.

3 TEST RESULTS

3.1 Introduction

A total of 81 discrete fibre tests were conducted; 57 were uniaxial tensile tests and 24 were direct shear tests. The results of the uniaxial tensile (UT) and direct shear (DS) tests are presented in Sections 3.2 and 3.3 respectively.

3.2 Uniaxial tensile (UT) tests

The load versus separation plane opening displacement results are presented in Figures 3 to 8. Figures 9 and 10 show the relationship between fibre inclination angles and peak load in the discrete fibre pullout tests. Figures 11 and 12 show the relationship between fibre inclination angles and fibre pullout energy in discrete fibre pullout tests. In Table 5 survey of the observed failure modes is performed for the discrete fibre uniaxial tensile tests.

Table 5. Survey of discrete fibre failure for UT tests.

Fibre inclination angle, θ (degree)	Failure Mode UTD±θEH-				UTD±θST-	
	M (25)	M (35)	G (35)	R (25)	M (23)	G (28)
0	P	P	F/P	F/P	P	P
15	-	-	F/P	F	-	P
30	P	P	F/P	F	P	P
45	-	-	F	F	-	F/P
60	P	P	F	F	P	F/P

Note: * F = fibre fracture; P = fibre pullout
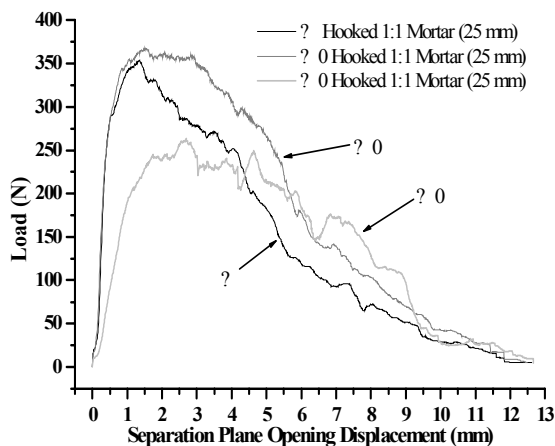
Figure 3. Average load versus separation plane opening displacement for UT±θEH-M (25).
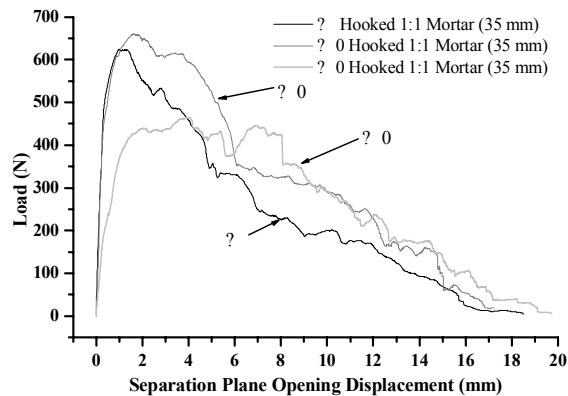
Figure 4. Average load versus separation plane opening displacement for UT±θEH-M (35).
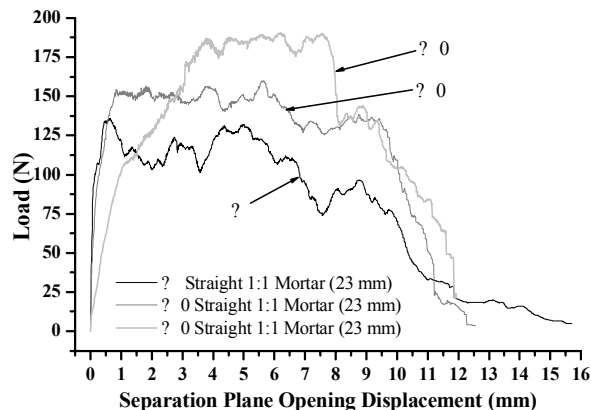
Figure 5. Average load versus separation plane opening displacement for UT±θST-M (23).
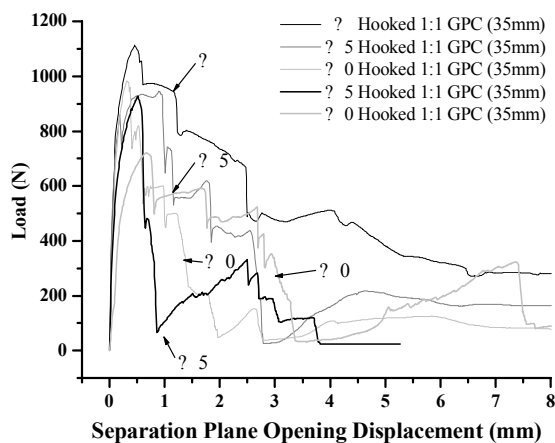
Figure 6. Average load versus separation plane opening displacement for UT±θEH-G (35).
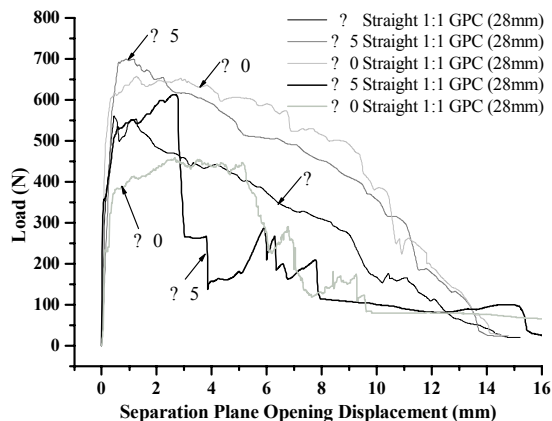
Figure 7. Average load versus separation plane opening displacement for UT±θST-G (28).
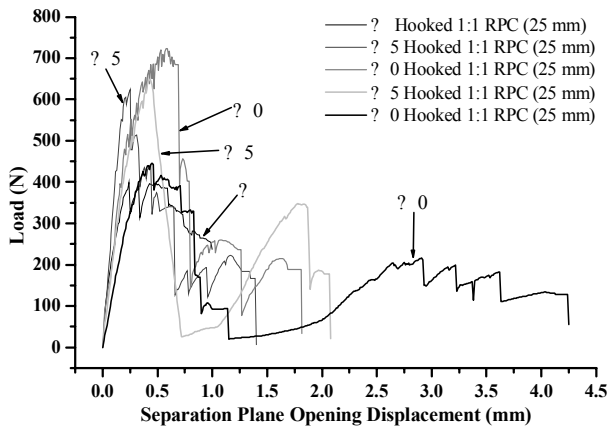
Figure 8. Average load versus separation plane opening displacement for UT±θEH-R (25).
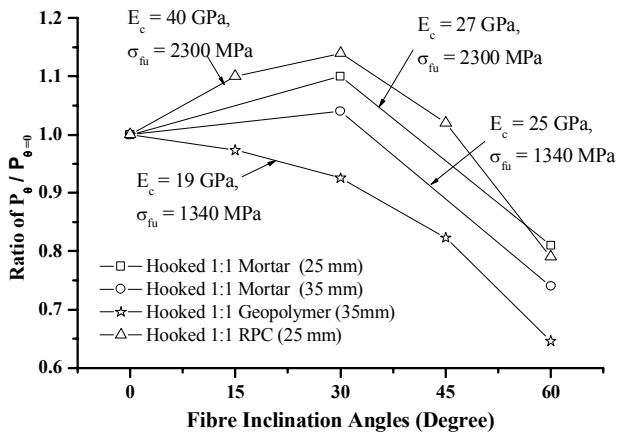
Figure 9. Plot of ratio of peak load at inclination angles to peak load at aligned versus fibre inclination angles for EH fibre subjected to uniaxial tensile action.
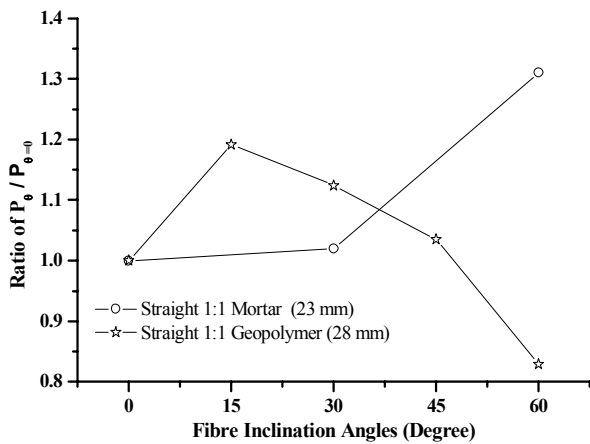
Figure 10. Plot of ratio of peak load at inclination angles versus fibre inclination angles to peak load at aligned for ST fibre subjected to uniaxial tensile action.

Table 6. Survey of discrete fibre failure for DS tests.

Fibre inclination angle, θ (degree)	Failure Mode UTD±θEH-G(35)	UTD±θST-G(28)
+30	F	P
0	F	F/P
-15	F	F
-30	F	F
-45	F	F
-60	F	F

Note: * F = fibre fracture; P = fibre pullout
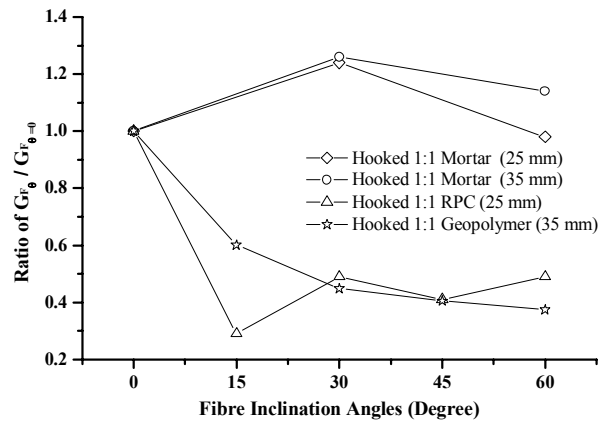
Figure 11. Plot of ratio of pullout energy at inclination angles to pullout energy at aligned versus fibre inclination angle for EH fibre subjected to uniaxial tensile action.
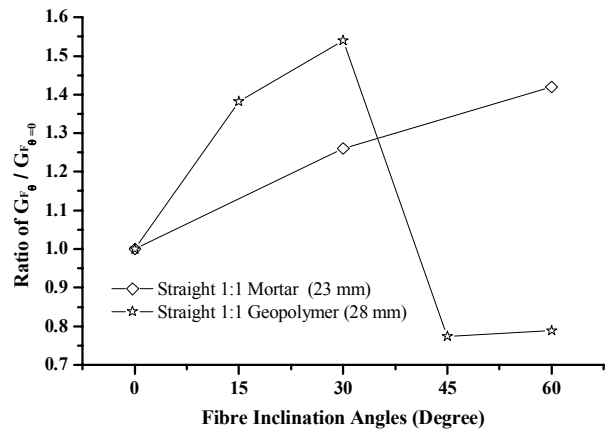
Figure 12. Plot of ratio of pullout energy at inclination angles to pullout energy at aligned versus fibre inclination angle for ST fibre subjected to uniaxial tensile action.

3.3 Direct shear (DS) tests

Figures 13 and 14 shows the load versus separation plane displacement results for EH and ST fibres at various inclination angles. The peak load and the sliding displacement at 90% of the peak load determined for each test are presented in Figures 15 and 16. The survey of the observed failure modes is tabulated in Table 6.
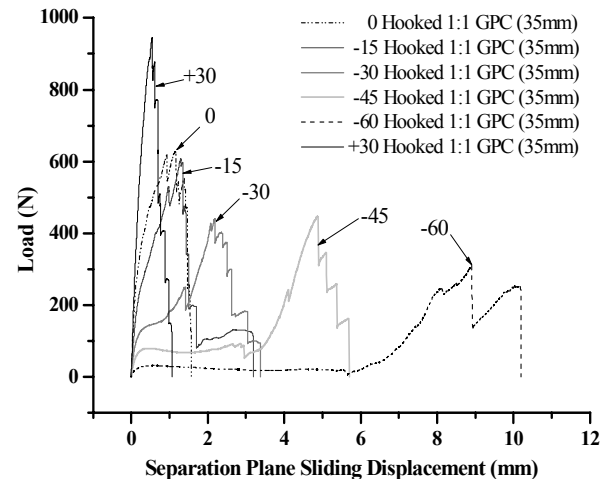
Figure 13. Average load versus separation plane sliding displacement for DS±θEH-G (35).

1508
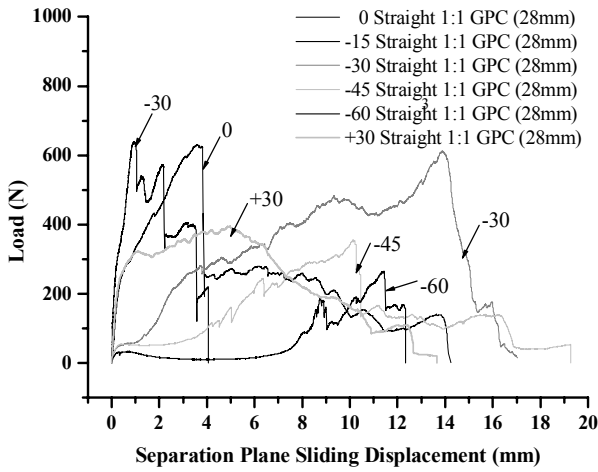
Figure 14. Average load versus separation plane sliding displacement for DS±θST-G (28).
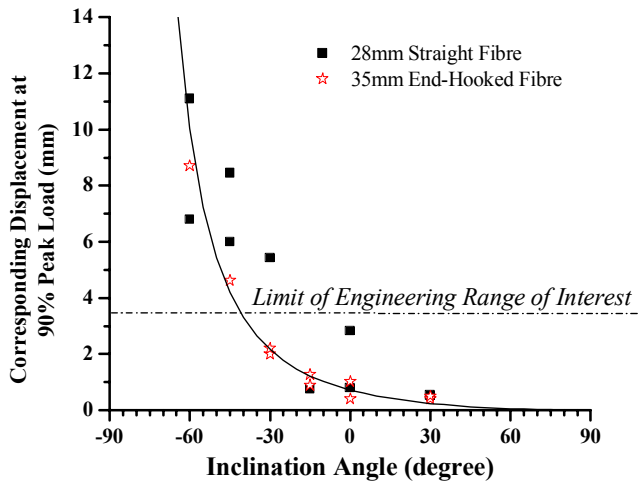
Figure 15. Separation plane sliding displacement at 90% peak load versus fibre inclination angle for DS±θEH-G (35) and DS±θST-G (28).
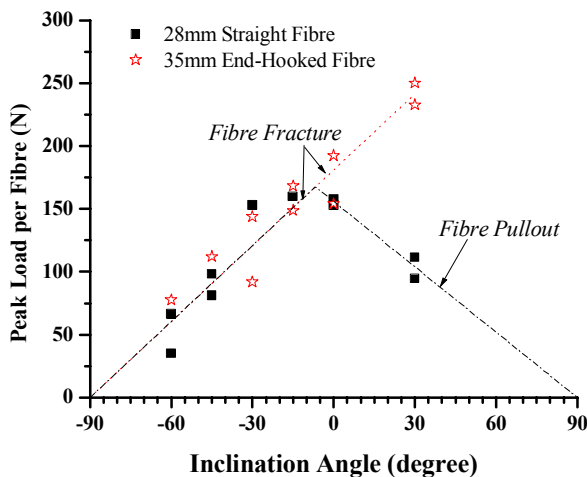
Figure 16. Plot of peak load per fibre versus fibre inclination angles for DS±θEH-G (35) and DS±θST-G (28) subjected to direct shear action.

4 ANALYSIS OF RESULTS

For both uniaxial tensile and direct shear tests, the discrete fibre failed in one of three mode modes: fibre pullout, fibre fracture or combination of the two.

4.1 Mode I fracture behaviour

Comparing Figures 3 to 8, different steel fibre types have different micro-mechanisms in the pullout process. For 0° inclination angle, initially both the ST and EH fibres and the surrounding matrix deform elastically. In this stage the fibre remains fully bonded to the matrix. As the applied load increases, debonding at the fibre-matrix interface takes place and debonding propagates over the length of the fibre. For ST fibres (UT±θST series), slippage or frictional pullout occurs until the fibre is completely pulled through the fibre tunnel, where the fibre tunnel is the space was previously occupied by the fibre. In the case of EH fibres (UT±θEH series), a mechanical clamping is introduced and much of the pullout resistance is required to overcome the mechanical anchorages and straighten the fibres.

In Figures 9 and 10, the values of the maximum pullout load are given relative to the maximum pullout load of a fibre aligned at 0°. The bonding properties of EH steel fibres (Fig. 9) increase to a maximum and decrease again as the angle between the fibre and the load direction increases. Even at the high inclination angles of 60°, there is an insignificant difference comparing the angled fibres to the aligned fibres, except in the case of fibres being pulled out from geopolymer concrete where the peak load decreases as the fibre inclination angles increase. The initial increase in peak load in cement based matrix is mainly due to the increase in the fibre inclination angles from being aligned to the loading direction that result in bending of the fibre through the fibre channel and, consequently, a slight increase in the peak pullout load was observed due to additional anchorage that is provided through snubbing. As the inclination fibre angle increases, the bond through snubbing increases until the stage where the fibres begin to fracture.

Generally, in the case of ST steel fibre pulled out from conventional cement matrix (Fig. 10), the bond-slip characteristics of inclined fibres were superior to those of fibres aligned with respect to the loading direction. In the case of high strength geopolymer concrete, however, as the inclination angle increases, the peak load increases. This can be seen in Figure 10 for fibre inclination angle up to approximately 30°. For the ST steel fibres, the snubbing effect becomes more influential as the fibre inclination angles increases, resulting an increase in peak pullout load. For the geopolymer concrete, the effect of increased frictional stress and bending stress due to snubbing causes the fibres to fracture for fibre inclination angle beyond 30°.

In addition, it is apparent that the efficiency of fibres pullout is influenced by the elastic modulus of the pullout medium (Fig. 9). As the modulus and, hence, the stiffness of the matrix surrounding the fibres increases, the deformability resistance increases

and the tendency of the fibres to "cut through" the matrix decreases. As a consequence, the snubbing resistance increases giving a higher pullout efficiency. Also noticeable in Figure 9 is that the pullout efficiency increases with increasing fibre strength.

Greater energy is required to overcome pullout resistance of the fibre for increasing fibre angles (Figs. 11 and 12), as has been demonstrated by many researchers. For example, Htut & Foster (2007, 2008) showed in their radiographic observations on the fibre pullout process that the snubbing length is a function of fibre inclination angle.

Comparing the various EH fibres pulled out from cement mortar in Figure 11, the fibre pullout energy increases as the fibre angle increased from 0° to approximately 30°, and then decreased beyond $\theta = 30°$. This slight increase in peak pullout load, as well as fibre pullout energy, is attributed to the additional mechanical bond due to snubbing. However, as the fibre inclination angle continues to increase, the matrix spalls around the snubbing zone and the peak load in the fibre corresponds to a significant increase in separation plane opening displacement, with less of the fibre embedded in the matrix. Matrix spalling, due to fibre being abraded against the edge of the separation plane, leads to a reduction in the pullout resistance. In addition, fibres may fracture at high fibre inclination angles due to high stress concentrations as the result of fibre bending and may lead to lower pullout energy. In the case of fibres being pulled out from RPC and geopolymer concrete, a significant decrease in pullout energy occurs if the fibre fractures. This behaviour is brittle and significantly reduces the load carrying capacity and highlights the disadvantage of using EH fibres in high strength cementitious composites.

For the RPC and geopolymer concrete (UT±0EH-G (25) and UT±0EH-R (25) series), some fibres are fractured while some are pulled out. By observation (Table 5) it appears that the critical length is similar or somewhat near that of the fibre length used in RPC and geopolymer concrete. In this case, the average bond strengths can be calculated as

$$\tau_b = d_f \sigma_{fu} / (2l_c) \tag{1}$$

where l_c = critical fibre length; d_f = diameter of fibre; and σ_{fu} = ultimate tensile strength of the fibre. The bond strengths of the RPC and geopolymer concrete were found to be $2.3f_{ct}$ and $2.2f_{ct}$ respectively, where f_{ct} is the uniaxial tensile strength of the concrete matrix without fibres and is taken as $0.5\sqrt{f_{cm}}$, in which f_{cm} = mean cylinder compressive strength.

Generally, in the case of the ST steel fibres in Figure 12, bond-slip characteristics of inclined fibres are significantly superior to those that are aligned with respect to the loading direction. For the ST steel fibres, the snubbing effect becomes more influential as the fibre inclination angle increases, resulting in an increase in the pullout load and, consequently, more pullout energy is required to bend the fibre. A similar trend was observed in the case for geopolymer concrete up to fibre inclination angles of 30°.

4.2 Mode II fracture behaviour

Figures 13 and 14 show the initial elastic response for the EH and ST fibres with positive inclination angles is reasonably linear. The debonding process occurs as the applied load increases. For ST fibres (DS±θST series), the fibres were pulled out at fibre angles greater than 0°. Fibres angles at less than 0° fracture as a result of snubbing effects. This is likely as negative fibre inclination angles produce acute angles at the separation place surface and increase the influence of bending stress on the fibres. Similar behaviour was also reported by Lee & Foster (2006a) on discrete fibre direct shear test on ordinary cement concrete.

Similar to mode I fracture, the anchorage provided by EH fibres (DS±θEH series) results in the fracture of fibres. As shown in Figure 13, after a fibre fractures, there is a sudden drop in the load. This failure is brittle and is highly undesirable.

In Figure 15, for both ST and EH fibres, longer sliding displacement at peak load can be seen as the fibre inclination angle becomes more negative. A similar observation was made by Lee & Foster (2006b). Localised damage to the cementitious matrix due to snubbing effect occurs before the fibres are engaged and pick up the load. This further confirms that in a fibre composite subjected to Mode II behaviour, only those fibres at high positive angles are likely to be effective in carrying load over the engineering range of a few millimetres. That is, half or more of the fibres do not carry load efficiently.

5 CONCLUSIONS

Based on the experimental work and the analysis of results of the tests presented in this paper, the following conclusions are drawn:

1. Snubbing effect dominates the highly inclined fibres for Mode I and negatively inclined fibres for Mode II. An initial increase in both the pullout energy and peak load is expected for both EH and ST fibres pullout from conventional cement mortar matrix.

2. Fibres at high inclination angles potentially fracture and, consequently, result in a brittle response.

3. The fibre pullout efficiency is depended on the modulus of the pullout medium and the tensile strength of the fibres. It is evident that although geopolymer concrete had a higher compressive strength

than the conventional mortar tested in this study, the pullout efficiency of the geopolymer was lower due to its lower elastic modulus.

4. In high strength cementitious composites such as the geopolymer concrete used in this study and RPC, fibre fracture is common where EH fibres are used, due to the highly efficient bond between matrix and fibres and the mechanical anchorage provided by snubbing and in the hook. This highlights the disadvantage of using EH fibres in a high strength matrix.

5. On the other hand, without end-hooks questions arise as to the performance under longitudinal shear (Mode II) forces.

REFERENCES

Bartos, P. J. M. & Duris, M., 1994. Inclined tensile strength of steel fibres in a cement-based composite. *Composites* 25 (10), pp. 945-952.

Foster, S. J., Lee, G. G. & Htut, T. N. S., 2007. "Radiographic imaging for the observation of Modes I and II fracture in fibre reinforced concrete". *The 6th International Conference on Fracture Mechanics of Concrete and Concrete Structures*, Taylor & Francis, pp. 1457-1465.

Gopalaratnam, V. S. & Shah, S. P., 1987. Tensile failure of steel fibre reinforced mortar. *Journal of Engineering Mechanics* 113(5). pp. 635-652.

Gourley, J.T. & Johnson, G.B., 2005. Developments in geopolymer precast concrete. *Proceeding of the fourth World Congress Geopolymer*, France, pp. 133-137.

Guerrero, P. & Naaman, A. E., 2000. Effect of mortar fineness and adhesive agents on pullout response of steel fibres. *ACI Materials Journal* 97(1), pp. 12-20.

Hardjito, D. & Rangan, B.V., 2005. Development and Properties of Low Calcium Fly Ash Based Geopolymer Concrete". *Research Report GC 1*, Curtin University of Technology, Perth, Australia: 93pp.

Htut, T. N. S. & Foster, S.J., 2007. X-ray Imaging for the Observation of Mode I Fracture in Fibre Reinforced Concrete In Veidt, Martin (Ed), *Proceedings of the 5th Australasian Congress on Applied Mechanics*, Brisbane, Qld, Engineers Australia, pp. 120-125.

Htut, T. N. S. & Foster, S. J., 2008. Behaviour of steel fibre reinforced mortar and concrete in tension. In Aravinthan, T., Karunasena, W. & Wang, H. (Eds.), *Futures in Mechanics of Structures and Materials*, Toowoomba, Australia, Taylor & Francis, pp. 33-38.

Lee, G. G. & Foster, S. J., 2006a. Behaviour of steel fibre reinforced mortar in Shear II: Gamma Ray imaging. *Report No. UNICIV R-445,* School of Civil & Environmental Engineering, The University of New South Wales.

Lee, G. G. & Foster, S. J., 2006b. Behaviour of steel fibre reinforced mortar in Shear I: Direct shear testing. *Report No. UNICIV R-444*, School of Civil & Environmental Engineering, The University of New South Wales.

Li, V. C., 1992. Postcracking scaling relations or fibre reinforced cementitious composites. *Journal of Materials in Civil Engineering*, ASCE, 4(1), pp. 41-57.

Li, Z., Ding, Z. & Zhang, Y., 2004. Development of Sustainable Cementitious Materials. *International Workshop on Sustainable Development and Concrete Technology*, Beijing, China, May 20-21.

Morton, J. & Groves, G. W., 1974. The cracking of composites consisting of discontinuous ductile fibres in a brittle matrix-effect of fibre orientation. *Journal of Materials Science* 9 (9), pp. 1436-1445.

Naaman, A. E. & Najm, H. 1991. Bond-slip mechanisms of steel fibres in concrete. *ACI Materials Journal*, 88(2), pp.135-145.

Robins, P., Austin, S. & Jones, P. 2002. Pullout behaviour of hooked steel fibres. *Materials and Structures/Materiaux et Constructions* 35(251), pp. 434-442.

Voo, J. Y. L. & Foster, S. J., 2003. Variable engagement model for fibre reinforced concrete in tension. *Report No. UNICIV R-420,* School of Civil & Environmental Engineering, The University of New South Wales.

Voo, J. Y. L. & Foster, S. J., 2004. Tensile-fracture of fibre-reinforced concrete: Variable engagement model In Di Prisco, M., Felicetti, R. & Plizzari, G. A. (Eds.), *Sixth RILEM Symposium on Fibre-Reinforced Concrete (FRC) - BEFIB 2004*, Varenna, Italy, RILEM, pp. 875-884.

Wallah, S.E. & Rangan, B.V., 2006. Low Calcium Fly Ash based Geopolymer Concrete: Long-term Properties. *Research Report GC 2*, Curtin University of Technology, Perth, Australia: 97pp.